

Sequential formation of analyte ions originated from bulk alloys for ambient mass spectrometry analysis

Jiaquan Xu, Teng-Gao Zhu, Konstantin Chingin, Yuhui Liu, Hua Zhang, and Huanwen Chen

Anal. Chem., **Just Accepted Manuscript** • DOI: 10.1021/acs.analchem.8b04309 • Publication Date (Web): 08 Nov 2018

Downloaded from <http://pubs.acs.org> on November 10, 2018

Just Accepted

“Just Accepted” manuscripts have been peer-reviewed and accepted for publication. They are posted online prior to technical editing, formatting for publication and author proofing. The American Chemical Society provides “Just Accepted” as a service to the research community to expedite the dissemination of scientific material as soon as possible after acceptance. “Just Accepted” manuscripts appear in full in PDF format accompanied by an HTML abstract. “Just Accepted” manuscripts have been fully peer reviewed, but should not be considered the official version of record. They are citable by the Digital Object Identifier (DOI®). “Just Accepted” is an optional service offered to authors. Therefore, the “Just Accepted” Web site may not include all articles that will be published in the journal. After a manuscript is technically edited and formatted, it will be removed from the “Just Accepted” Web site and published as an ASAP article. Note that technical editing may introduce minor changes to the manuscript text and/or graphics which could affect content, and all legal disclaimers and ethical guidelines that apply to the journal pertain. ACS cannot be held responsible for errors or consequences arising from the use of information contained in these “Just Accepted” manuscripts.

Sequential formation of analyte ions originated from bulk alloys for ambient mass spectrometry analysis

Jiaquan Xu¹, Tenggaio Zhu¹, Konstantin Chingini¹, Yuhui Liu², Hua Zhang³ and Huanwen Chen^{1*}

¹Jiangxi Key Laboratory for Mass Spectrometry and Instrumentation, East China University of Technology, Nanchang, P. R. China. ²State Key Laboratory Breeding Base of Nuclear Resources and Environment, East China University of Technology, Nanchang 330013, P. R. China. ³ State Key Laboratory of Inorganic Synthesis and Preparative Chemistry, College of Chemistry, Jilin University, Changchun, 130012, PR China

ABSTRACT: Rapid chemical decoding of bulk alloys to obtain both organic and elemental composition is of sustainable interest in multiple disciplines. Herein, an analytical strategy inherited from electrochemistry and mass spectrometry (MS) was developed for direct molecular characterization of alloys. While the organics on the alloy surface were simply extracted into the solvent for ESI-MS analysis, the components in the bulk alloy were successively converted into metal ions at appropriate electrolysis potentials, which were online chelated with specific ligands for ESI-MS analysis. A single sample analysis took only few seconds since no other sample pretreatment was required, and a detection limit of 0.1 ppb was achieved for a component in alloy with low sample consumption (< 1.0 mg). Proof-of-concept application indicated that the presented method has unique capability for successive analysis of organic and metallic components in liquids (e.g., engine oil), solids (e.g., alloy) and tunable spatial resolution (~1.0 - 1.0 × 10⁻⁵ cm²) for molecular characterization of bulk alloys.

Alloys contain at least one metal element, and are ubiquitous materials available in virtually any type of modern products including the fillings in teeth,¹⁻² the wheels on cars³⁻⁴ and the space satellites,⁵⁻⁶ etc. The property of alloys varies dramatically along with their elemental compositions,⁷ particularly for the alloys which are made up of multiple metal elements.⁸ In material science and engineering, tuning the elemental composition may control the function of alloys, leading to new functional materials.⁷⁻⁸ In mechanical industry, alloy particles in the lubricating oil or exhaust gas are useful indicators of the engine conditions.⁹⁻¹⁰ In manufacturing industry, the elemental composition of alloy is a useful quality index.⁷⁻⁸ Thus the rapid characterization of alloys to obtain the elemental composition is of sustainable interest in multiple disciplines, including life science,¹¹ material science,¹² mechanical industry¹³ and biological engineering.¹⁴

To date, alloys are normally dissolved using various chemical reagents to form analyte solutions prior to elemental analysis. The sample solutions are usually offline analyzed by either atomic emission spectrometry (AES),¹⁵ atomic absorption spectrometry (AAS)¹⁶ or inductively coupled plasma mass spectrometry (ICP-MS).¹⁷ The offline procedures render a significantly long time for sample manipulation and pretreatment,¹⁸ resulting in a low analytical throughput. Laser ablation inductively coupled plasma mass spectrometry (LA-ICP-MS) or laser ablation electrospray ionization mass spectrometry have been attempted for online alloy analysis,¹⁹ but requiring expensive high energy laser generator and hard-to-reach standards for quantitative analysis. No matter the alloy is online or offline treated, ICP-MS provides only elemental information due to the highly energetic ionization process occurring inside the ICP torch.¹⁷ Ideally, soft ionization is preferable for mass spectrometry analysis of alloys, particularly in the cases where the organics on the alloy surface are of analytical interest.²⁰

Herein, electrochemical ionization mass spectrometry (ECI-MS) was developed to directly characterize alloys at the molecular levels without tedious sample pretreatment, for which sequential formation of metal ions of bulk alloys via

electrolysis was a crucial step. As schematically shown in Figure 1, charged electrolytic solution (e.g., H₂O/CH₃CN, 1:1, v/v) was injected at 2.0 μL/min by a syringe pump to flow through a 50 μL fluid tight micro electrolytic cell (MEC), inside which the organic chemical species on the alloy surface took the precedence over the rest material to be extracted into the solution. Once the metal was exposed to the solution, a potential (e.g., 1.0 V) was applied to the working electrode inside the MEC. Consequentially, the elemental components were successively converted into the corresponding metal ions by tuning the electrolysis potentials, ensuring the high selectivity and specificity for metal ion generation.²¹ Note that the electrolysis potential was floated on the ESI voltage (±3.0 kV), such that the ESI high voltage brought no interference to the electrolysis.²²⁻²³ Once the metal ions were formed, they reacted immediately with specific organic ligands added in excess into electrolyte solvent to form metal-organic complexes, which were carried by the solvent flow towards the outlet of the MEC to produce ambient ions, with the assistance of the pneumatic system and the electric field, for mass analysis using a LTQ-Orbitrap-MS instrument.

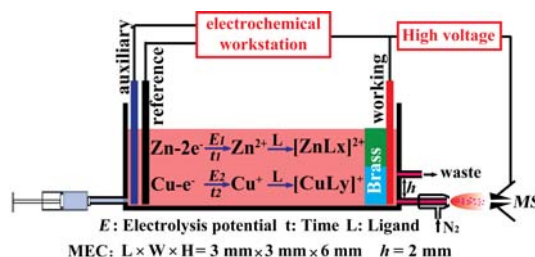


Figure 1 Schematic illustration of the ECI-MS method for analysis of alloys

EXPERIMENTAL SECTION

Construction of ECI-MS device: The analysis device consisted of a MEC (about 50 μL), a nebulization system and a mass spectrometer. The MEC employed two platinum wire (Diameter = 500 μm) as working electrode and auxiliary electrode, Ag/AgCl as reference electrode, respectively. In

order to ensure the reproducibility of experimental behavior and to avoid the need for the cleaning of electrode surface, a new disposable MEC unit was assembled and used in every experiment. Metal was connected to anode or acted as a bipolar electrode placed between two platinum wire.²⁴ Electrolyte was injected into the MEC by a pump. During the detection of metal materials, a potential (E) floated on +3 KV high voltage was applied to working electrode by CHI 660D electrochemical workstation. When potential E is high enough to meet the requirement of metal electrolysis, metal would transform into metallic ions. Then, the electrolyte contained metal ions were sprayed into MS by pneumatic nebulization for analysis. The distance between spray emitter and entrance of MS is 1.0 cm.

ECI-MS analysis of metallic materials: As shown in Figure 1, a piece of alloy (e.g. 1 mm × 1 mm × 0.1 mm) was placed in the MEC, then a potential was applied to the working electrodes. Several kinds of electrolyte were used for metals electrolysis, including H₂O, H₂O/CH₃CN (v/v 1/1), H₂O/CH₃CN (v/v 1/1) with 0.1 mM Phen (H₂O/CH₃CN/Phen), and H₂O/CH₃CN (v/v 1/1) with 0.1 mM EDTA (H₂O/CH₃CN/EDTA). After the electrolyte was injected into the MEC at a flow rate of 2 μL/min, the electrolysis would be triggered to produced metal ions which would be carried by the electrolyte and sprayed into the MS for analysis. A LTQ-orbitrap-MS was used for the MS analysis.

RESULTS AND DISCUSSION

ECI-MS features the successive characterization of organic compounds and metallic components by tuning the electrolysis potential. Given a brass exposed to atmospheric aerosols containing glycine as the labeling marker, the organic species (e.g., glycine) were immediately dissolved when the brass soaked into the CH₃OH electrolyte and detected as protonated molecules (the peak assignment except for glycine was not attempted), among which the glycine showed up at *m/z* 76 [Gly+H]⁺ with high abundance (Figure 2a). Note that ambient ionization techniques including DESI/DAPCI/DART detected the organic species including the glycine, but no metal ions were observed during the ambient ionization experiments (Figure S1). For ECI-MS, a specific metal such as Zn, Cu generated the ions as usual (black and blue line in Figure 2b) by electrolysis. The components in alloy were converted into metal ions successively (red line in Figure 2b) at differential potentials. Thus, once the glycine run out (no signal of organic species detectable), a scanning potential (-1~1 V, powered by an electrochemical workstation) was applied to the working electrode floated on +3 KV to enable the electrolysis of metallic components. Figure 2c illustrates that the signal of Zn and Cu appeared at -0.65 V and 0 V, respectively, and the intensity increased with the potential shift to positive. The feature enabled the sensitive detection of trace Zn (100 ppb) in Zn/Cu alloy with molecular specificity (Figure S2).

Figure 3 shows the nonnegligible contribution of the organic ligands on the abundance of mass spectral signals. For example, with precise mass measurements, the relatively weak signals of [Cu+2(H₂O)]⁺, [Cu+3(H₂O)]⁺, [Cu+6(H₂O)]⁺ were detected using H₂O as the electrolyte with +1.0 V applied to the Cu sample (Figure 3a), while dominant signals of Cu (Figure 3b) were detected as [Cu+2(CH₃CN)]⁺, [Cu+H₂O+CH₃CN]⁺ and [Cu+CH₃CN]⁺ using H₂O/CH₃CN (v/v 1:1) as the electrolyte, with a signal-to-noise (S/N) ratio

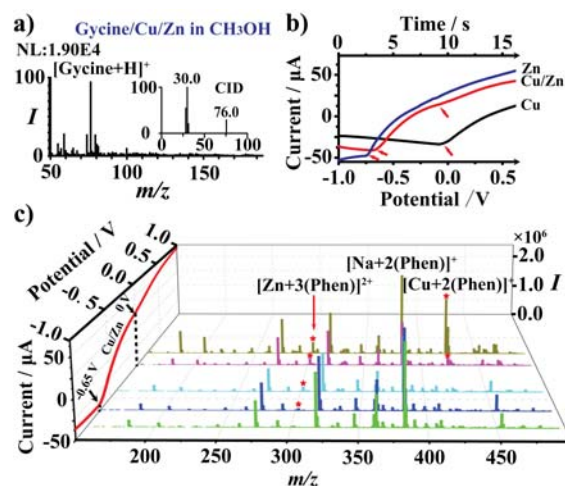


Figure 2 Successive analysis of glycine covered brass. a) ECI-MS spectrum of glycine covered brass in H₂O/CH₃CN; b) Electrolysis current curve of Cu, Zn and brass during -1 ~ 1 V with potential scanning rate of 0.1 V/s. The points marked by red arrows were the starting point of metal electrolysis; c) ECI-MS spectrum of brass obtained under various electrolysis potential (-0.85 V, -0.6 V, -0.4 V, 0 V and 0.2 V) in H₂O/CH₃CN/Phen. The dominant peak assignments: *m/z* 76.0391 [Glycine+H]⁺; *m/z* 302.0674 [Zn+3(Phen)]²⁺; *m/z* 383.1265 [2(Phen)+Na]⁺; *m/z* 423.0658 [Cu+2(Phen)]⁺.

improved about 10 times. Furthermore, when phenanthroline (Phen) was added into the H₂O/CH₃CN (v/v 1:1) solution, signals of [Cu+2(CH₃CN)]⁺, [Cu+Phen]⁺, [Cu+Phen+CH₃CN]⁺ and [Cu+2(Phen)]⁺ were detected with increased abundances (Figure 3c), probably because Cu⁺ forms more stable complex with Phen (the stability constant of metal complexes lgKs=9.08)²¹ rather than CH₃CN (lgKs=3.9)²⁵ or H₂O.²⁶ Similar results were also found in Phen/H₂O or Phen/CH₃CN systems, where [Cu+Phen]⁺, [Cu+2(Phen)]²⁺ or [Cu+3(Phen)]²⁺ were much stronger than [Cu+2(CH₃CN)]⁺, [Cu+2(CH₃CN)]⁺ or [Cu+2(H₂O)]⁺ (Figure S3). More interestingly, for online analysis of Cu using H₂O/CH₃CN/Phen solution: the dead time was 0 - 0.5 min and the signal of [Cu+Phen]⁺ increased along the electrolysis time during 0.5 - 1.5 min, while the signal of [Cu+2(CH₃CN)]⁺ rapidly increased during 0.5 - 0.6 min and then decreased during 0.6 - 1.5 min (Figure 3d). The CH₃CN was around 10⁴ times more than Phen in the electrolyte, but the lgKs for [Cu+Phen]⁺ was about 10⁵ times more than that for [Cu+2(CH₃CN)]⁺. Consequently, large amount of [Cu+2(CH₃CN)]⁺ was rapidly formed by the reaction between Cu⁺ and large amount CH₃CN at beginning under a kinetics controlled process, and then decreased because of the competitive reaction between Phen and Cu⁺, while the amount of [Cu+Phen]⁺ increased with the reaction time since the reaction was under a thermodynamics controlled process due to the large lgKs. However, after 1.5 min, both the signal levels of [Cu+Phen]⁺ and [Cu+2(CH₃CN)]⁺ decreased drastically, while [Cu+2(Phen)]²⁺ rapidly increased (Figure 3d). This phenomenon was attributed to the fact that Cu⁺ ions were preferentially solvated by CH₃CN while Cu²⁺ was preferentially solvated by H₂O.²⁶ Thus, Cu⁺ would be oxidized to Cu²⁺ with the accumulation of Cu⁺ in MEC. Then, Cu²⁺ selectively reacted with Phen inside the MEC to form stable complex [Cu+2(Phen)]²⁺ (lgKs=16.0). Usually, Cu⁺ is instantly converted into Cu²⁺ in most media since the complex

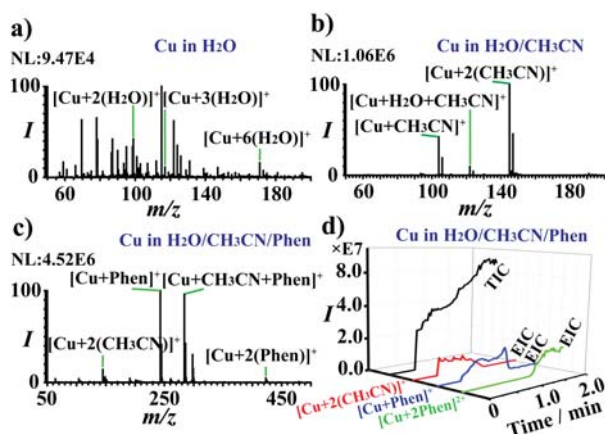


Figure 3 Mass spectra of Cu obtained by ECI-MS under different conditions. a) Cu in H₂O; b) Cu in H₂O/CH₃CN; c) Cu in H₂O/CH₃CN/Phen; d) Total ion chromatogram and extracted ion chromatogram of Cu signal obtained in H₂O/CH₃CN/Phen. The dominant peak assignments: *m/z* 98.9499 [Cu+2(H₂O)]⁺; *m/z* 116.9595 [Cu+3(H₂O)]⁺; *m/z* 170.9924 [Cu+6(H₂O)]⁺; *m/z* 103.9555 [Cu+CH₃CN]⁺; *m/z* 121.9661 [Cu+CH₃CN+H₂O]⁺; *m/z* 144.9821 [Cu+2(CH₃CN)]⁺; *m/z* 242.9976 [Cu+Phen]⁺; *m/z* 284.0241 [Cu+Phen+CH₃CN]⁺; *m/z* 211.5330 [Cu+Phen]⁺.

[Cu+2(Phen)]²⁺ is much more stable than [Cu+Phen]⁺.²⁷ The ECI-MS however created a possibility to observe this transient process with a time window width more than 1.5 min.²⁸ For the analysis of Zn and Fe, (Figure S4), the signal intensity levels were also affected by the ligands in the order as H₂O/CH₃CN/Phen > H₂O/CH₃CN > H₂O. For instance, using H₂O/CH₃CN/Phen instead of H₂O/CH₃CN as the electrolyte, the signals of Zn²⁺ and Fe²⁺ were enhanced more than one order of magnitude by forming [Zn+2(Phen)]²⁺, [Zn+3(Phen)]²⁺, [Fe+3(Phen)]²⁺ (Figure S4).

Unlike Cu, Zn and Fe, no signal of Al³⁺ was detected by ECI-MS in all of the three electrolyte (H₂O, H₂O/CH₃CN and H₂O/CH₃CN/Phen) under either positive or negative ion detection mode, because Al forms no stable complex with the ligands. Therefore, H₂O/CH₃CN/EDTA was employed as the electrolyte since Al-EDTA gives stable complex (lgKs=16.3), and strong signals of Al, Zn and Fe were obtained (Figure S5a-c) under the negative ion detection mode, while Cu was detected as [Cu+EDTA-4H]²⁻ and [Cu-EDTA-3H]⁻ since the Cu²⁺-EDTA complexes were highly stable (lgKs=18.8) (Figure S5d). These results demonstrated that the ligands were essential for metal analysis by forming metal-organic complexes.²⁹ Based on this strategy, a detection limit of 100 ppb Cu in a bulk Al (w/w) sample of high purity (99.9999%) was obtained in the positive ion detection mode, and 10 ppm Al in a bulk Cu sample (99.999%) was achieved in the negative ion detection mode (detailed in Figure S6). In comparison with the traditional methods (e.g., ICP-MS, ICP-AES), this method provided features such as reduced analysis time (<10 min), minimal sample consumption (<1 mg) and least sample pretreatment.

For quantitative analysis, the ECI-MS was experimentally calibrated using H₂O/CH₃CN/Phen solution spiked with different concentration levels of Cu²⁺ and Zn²⁺. As the result, the signals of [Cu+3(Phen)]²⁺ and [Zn+3(Phen)]²⁺ linearly responded to concentration over the range of 0.2 ppb - 200 ppb with a LOD of 0.1 ppb (S/N=3). As a demonstration, a piece

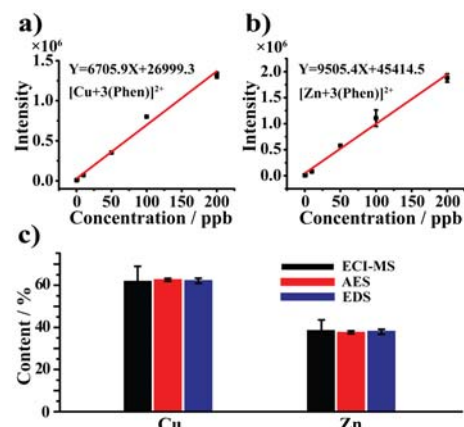


Figure 4 The quantitative performance of ECI-MS. Calibration curve of a) [Cu+3(Phen)]²⁺ and b) [Zn+3(Phen)]²⁺ prepared by ECI-MS; c) The component of brass obtained by ECI-MS, AES and EDS. (n=3).

of brass (1 mm × 1 mm × 0.1 mm) was analyzed in H₂O/CH₃CN/Phen, and the solution-phase metal concentration was calculated using the calibration curves as detailed in the Experimental section (see SI), providing the contents of Cu at 61.7% and Zn at 38.3% in 5 min (Figure 4c). The analytical results were validated in parallel using classic instrumental methods such as AAS and EDS (Figure 4c and Figure S7), showing the excellent agreement with each other.

High throughput and minimal invasion is highly demanding for metals analysis.³⁰ As the first attempt, a ceramic probe (or Si₃N₄ tip) with rigid tip was used for micro-area sampling. With a slight scratch, a tiny amount of metallic sample (about 7 μg, detailed in SI for estimation) was attached on the tip of the probe, leaving a mark about 0.6 × 0.07 mm on the brass sheet (inset in Figure 5a). The probe tip loaded with the tiny metal particles was immersed in the MEC (Figure 1) filled with H₂O/CH₃CN/Phen as the electrolyte.²⁴ To avoid potential interference, the sampling probe should be inert to electrolyzing. As the result, the Zn, Cu were both detected (Figure 5a) as [Zn+2(Phen)]²⁺, [Zn+3(Phen)]²⁺ and [Cu+2(Phen)]⁺, respectively, indicating that the components of the brass were successfully detected with a single sample loading. The spatial resolution of the method was about 1.0 × 10⁻⁵ cm² (detailed in SI) for alloys analysis. In contrast, a big surface was directly sampled by soaking the whole sample as the electrode or by scratching with a piece of abrasive paper for sampling, which enabled the direct elemental analysis of large area (Figure S8). Therefore, the data demonstrated that the ECI-MS technique was useful for either micro-area or big surface elemental analysis with high throughput and minimal invasion.

Experimental investigation of the metal particles in the engine oil was conducted for engine conditions control. In brief, 20 μL engine oil (being used for 4 months) and 20 μL 1 mM Phen aqueous solution were mixed together inside the MEC. In comparison with the ECI-MS spectrum (Figure S9) recorded using the fresh engine oil, many peaks attributed to the organic ingredients of the oil were directly detected in the mass spectrum (Figure S10), showing that the engine oil was partially degraded after being used for 4 months. Being applied with +1.0 V for electrolysis of 5 min, the under layer aqueous phase was directly electrospayed for MS analysis.

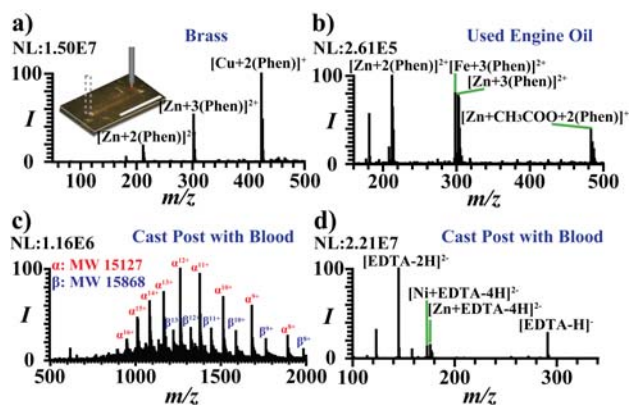


Figure 5 Application of ECI-MS for alloys analysis. a) Mass spectrum of brass which was sampled by scraping with a rigid tip. The inset is a picture of brass after sampling. The scale bar is 0.5 mm; b) Mass spectrum of metals in a used engine oil; c) Mass spectrum of blood adhered on a cast post; d) Mass spectrum of metals in a cast post obtained. The dominant peak assignments: m/z 181.0764 $[\text{Phen}+\text{H}]^+$; m/z 212.0330 $[\text{Zn}+2(\text{Phen})]^{2+}$; m/z 298.0706 $[\text{Fe}+3(\text{Phen})]^{2+}$; m/z 172.9934 $[\text{Ni}+\text{EDTA}-4\text{H}]^{2-}$; m/z 175.9902 $[\text{Zn}+\text{EDTA}-4\text{H}]^{2-}$; m/z 145.0343 $[\text{EDTA}-2\text{H}]^{2-}$.

Unlike the fresh engine oil, abundant signals corresponding to the ionic species of $[\text{Fe}+2(\text{Phen})]^{2+}$, $[\text{Zn}+2(\text{Phen})]^{2+}$, $[\text{Zn}+\text{CH}_3\text{COO}+2(\text{Phen})]^+$ were obviously observed in the mass spectrum (Figure 5b), suggesting that the used engine oil contained Fe and Zn at high levels. Accordingly, the engine abrasion could be evaluated by the concentrations of metal species in the engine oil without complex sample pretreatment.

Cast post is an important metallic unit in teeth repair. ECI-MS analysis of the cast post provides molecular information on both the elemental compositions and the biochemicals (e.g., metabolites, blood, etc) thereon. For example, characteristic signals of hemoglobin were detected from a used cast post using $\text{CH}_3\text{OH}/\text{H}_2\text{O}/\text{HCOOH}$ (50/50/1, v/v/v) as the extraction solution (Figure 5c). With a 1.0 V potential was applied to the working electrode using $\text{H}_2\text{O}/\text{CH}_3\text{CN}/\text{EDTA}$ as electrolyte, Ni and Zn were successively detected in the form of $[\text{Ni}+\text{EDTA}-4\text{H}]^{2-}$ and $[\text{Zn}+\text{EDTA}-4\text{H}]^{2-}$ (Figure 5d), although as claimed the product was fabricated with Ni/Cr alloy. Because tiny amounts of metal sample (ng levels) were converted into ions for MS characterization, the cast post had only negligible changes on its surface after ECI-MS analysis (Figure S11), suggesting that the cast post could be considered for practical usage once it passes the quality checking. Therefore, this method was useful for diagnosing of dental disease (e.g. pulpitis, apicitis) and evaluation of the quality of cast posts.⁵¹

CONCLUSION

In summary, electrolysis for metal sampling has been online combined with sensitive MS detection, featuring the method a unique capability for successive characterization of organic and metallic components in liquids (e.g., engine oil), solids (e.g., alloy, cast post) with the merits such as high selectivity, high specificity, high throughput and tunable spatial resolution for molecular characterization of bulk materials.

ASSOCIATED CONTENT

Supporting Information: Experimental description; Mass spectra of different metal obtained by ECI-MS in different

electrolyte; EDS results for brass; Estimation of the spatial resolution and the amount of brass used in Figure 5a; Mass spectrum of brass sampled by scratching with abrasive paper; Mass spectrum of metals and organic component in engine oil; SEM images of cast post before and after ECI-MS analysis.

AUTHOR INFORMATION

*Corresponding Author: chw8868@gmail.com

Notes: The authors declare no competing financial interest and no conflicts of interest.

ACKNOWLEDGMENT

This work was supported by the National Natural Science Foundation of China (no. 21705016, 21727812), Program for Changjiang Scholars and Innovative Research Team in University (PCSIRT) (no. IRT_17R20), Project of Jiangxi provincial Department of Education (no. GJJ160543), Science and Technology Planning Project at the Department of Science and Technology of Jiangxi Province (no. 20171ACB21046).

REFERENCES

- (1) Imbeni, V.; Kruzic, J. J.; Marshall, G. W.; Marshall, S. J.; Ritchie, R. O. The dentin-enamel junction and the fracture of human teeth. *Nat. Mater.* **2005**, *4*, 229-232.
- (2) King, P. A. Tooth surface loss: Adhesive techniques. *Brit. Dent. J.* **1999**, *186*, 321-326.
- (3) Das, S.; Engineering, A. Design and Weight Optimization of Aluminium Alloy Wheel. *Int. J. Sci. Res.* **2014**, *4*, 1-12.
- (4) Zhang, B.; Maijer, D. M.; Cockcroft, S. L. Development of a 3-D thermal model of the low-pressure die-cast (LPDC) process of A356 aluminum alloy wheels. *Mater. Sci. Eng. A* **2007**, *464*, 295-305.
- (5) Kumar, C. S.; Mayanna, S. M.; Mahendra, K. N.; Sharma, A. K.; Rani, R. U. Studies on white anodizing on aluminum alloy for space applications. *Appl. Surf. Sci.* **1999**, *151*, 280-286.
- (6) Goueffon, Y.; Mabru, C.; Labarrère, M.; Arurault, L.; Tonon, C.; Guigue, P. Mechanical behavior of black anodic films on 7175 aluminium alloy for space applications. *Surf. Coat. Tech.* **2009**, *108*, 22-27.
- (7) Leyens, C.; Peters, M. *Titanium and Titanium Alloys: Fundamentals and Applications*, Springer-Verlag, 2006.
- (8) Appel, H. F.; Paul, J. D. H.; Oehring, M. *Gamma Titanium Aluminide Alloys: Science and Technology*, Wiley-VCH, 2011.
- (9) Yaqub, M. F.; Gondal, I.; Kamruzzaman, J.; Loparo, K. A. Abrasion Modeling of Multiple-Point Defect Dynamics for Machine Condition Monitoring. *IEEE T. Reliab.* **2013**, *62*, 171-182;
- (10) Li, Q. Q.; Chen, M. J.; He, S. Z. The Application of Oil Analysis in Shield Machine Condition Monitoring. *Mech. Electr. Eng. Tech.* **2010**, *39*, 125-127.
- (11) Sperling, R. A. *Metallic Nanomaterials. Nanomaterials for the Life Sciences*, Band 1. Herausgegeben von Challa S. S. R. Kumar. *Angew. Chem. Int. Ed.* **2009**, *48*, 7289-7289.
- (12) Mañosa, L.; González-Alonso, D.; Planas, A.; Bonnot, E.; Barrio, M.; Tamarit, J. L.; Aksoy, S.; Acet, M. Giant solid-state barocaloric effect in the Ni-Mn-In magnetic shape-memory alloy. *Nat. Mater.* **2010**, *9*, 478-481;
- (13) Inoue, A.; Shen, B.; Koshiba, H.; Kato, H.; Yavari, A. R. Cobalt-based bulk glassy alloy with ultrahigh strength and soft magnetic properties. *Nat. Mater.* **2003**, *2*, 661-663.
- (14) Huebsch, N.; Mooney, D. J. Inspiration and application in the evolution of biomaterials. *Nature* **2009**, *462*, 426-432.
- (15) Pohl, P. Hydride generation – recent advances in atomic emission spectrometry. *TrAC Trends Anal. Chem.* **2004**, *23*, 87-101.
- (16) Ferreira, S. L. C.; Bezerra, M. A.; Santos, A. S.; Santos, W. N. L. D.; Novaes, C. G.; Oliveira, O. M. C. D.; Oliveira, M. L.; Garcia, R. L. Atomic absorption spectrometry – A multi element technique. *TrAC Trends Anal. Chem.* **2018**, *100*, 1-6.

- 1
2
3 (17) Beauchemin, D. Inductively coupled plasma mass spectrometry.
4 *Anal. Chem.* **2010**, *82*, 4786-4810.
- 5 (18) Kelly, W. R.; Murphy, K. E.; Becker, D. A.; Mann, J. L.
6 Determination of Cr in certified reference material HISS-1, marine
7 sediment, by cold plasma isotope dilution ICP-MS and INAA:
8 comparison of microwave versus closed (Carius) tube digestion. *J.*
9 *Anal. Atom. Spectrom.* **2003**, *18*, 166-169.
- 10 (19) Huang, R.; Quan, Y.; Li, L.; Lin, Y.; Hang, W.; He, J.; Huang, B.
11 High irradiance laser ionization orthogonal time-of-flight mass
12 spectrometry: A versatile tool for solid analysis. *Mass Spectrom. Rev.*
13 **2011**, *30*, 1256-1268
- 14 (20) Lamaka, S. V.; Zheludkevich, M. L.; Yasakau, K. A.; Montemor,
15 M. F.; Ferreira, M. G. S. High effective organic corrosion inhibitors
16 for 2024 aluminium alloy. *Electrochim. Acta* **2007**, *52*, 7231-7247.
- 17 (21) Felder, D.; Nierengarten, J. F.; Barigelletti, F.; Ventura, B.;
18 Armaroli, N. Highly luminescent Cu(I)-phenanthroline complexes in
19 rigid matrix and temperature dependence of the photophysical
20 properties. *J. Am. Chem. Soc.* **2001**, *123*, 6291-6299.
- 21 (22) Zhou, F.; Berkel, G. J. Electrochemistry Combined Online with
22 Electro spray Mass Spectrometry. *Anal. Chem.* **1995**, *67*, 3643-3649;
- 23 (23) Brink, F. T.G. V. D.; Olthuis, W.; Berg, A. V. D.; Odijk, M.
24 Miniaturization of electrochemical cells for mass spectrometry. *TrAC*
25 *Trends Anal. Chem.* **2015**, *70*, 40-49.
- 26 (24) Chow, K. F.; Mavr , F.; Crooks, J. A.; Chang, B. Y.; Crooks, R.
27 M. A Large-Scale, Wireless Electrochemical Bipolar Electrode
28 Microarray. *J. Am. Chem. Soc.* **2009**, *131*, 8364-8365.
- 29 (25) Manahan, S. E.; Iwamoto, R. T. Complexes of copper(I) and
30 silver(I) with acetonitrile in water, the lower alcohols, acetone, and
31 nitroethane. *J. Electroanal. Chem.* **1967**, *14*, 213-217.
- 32 (26) Deng, H.; Kebarle, P. Bond Energies of Copper Ion-Ligand L
33 Complexes CuL₂⁺ Determined in the Gas Phase by Ion-Ligand
34 Exchange Equilibria Measurements. *J. Phys. Chem. A* **1998**, *102*, 571-
35 579.
- 36 (27) Kempen, E. C.; Brodbelt, J. S. A Method for the Determination
37 of Binding Constants by Electrospray Ionization Mass Spectrometry.
38 *Anal. Chem.* **2000**, *72*, 5411-5416.
- 39 (28) Brown, T. A.; Chen, H.; Zare, R. N. Detection of the Short-Lived
40 Radical Cation Intermediate in the Electrooxidation of N,N-
41 Dimethylaniline by Mass Spectrometry. *Angew. Chem. Int. Ed.* **2015**,
42 *54*, 11183-11185.
- 43 (29) Leize, E.; Jaffrezic, A.; Van Dorsselaer, A. Correlation Between
44 Solvation Energies and Electrospray Mass Spectrometric Response
45 Factors. Study by Electrospray Mass Spectrometry of Supramolecular
46 Complexes in Thermodynamic Equilibrium in Solution. *J. Mass*
47 *Spectrom.* **1996**, *31*, 537-544.
- 48 (30) Song, K.; Park, Y.; Kim, W. Application of non-resonant laser
49 ionization mass spectrometry for a fast isotope analysis of metal
50 microparticles. *Int. J. Mass spectrom.* **2006**, *254*, 122-126.
- 51 (31) Johnson, B. R.; Remeikis, N. A.; Van Cura, J. E. Diagnosis and
52 treatment of cutaneous facial sinus tracts of dental origin. *J. Am. Dent.*
53 *Assoc.* **1999**, *130*, 832-836.
- 54
55
56
57
58
59
60

1
2
3
4
5
6
7
8
9
10
11
12
13
14
15
16
17
18
19
20
21
22
23
24
25
26
27
28
29
30
31
32
33
34
35
36
37
38
39
40
41
42
43
44
45
46
47
48
49
50
51
52
53
54
55
56
57
58
59
60

for TOC only

